# Slow electron velocity-map imaging spectroscopy of the 1-propynyl radical

Jia Zhou and Etienne Garand
*Department of Chemistry, University of California, Berkeley, California 94720*

Wolfgang Eisfeld
*Theoretical Chemistry, Bielefeld University, D-33615 Bielefeld, Germany*

Daniel M. Neumark[a)]
*Department of Chemistry, University of California, Berkeley, California 94720*
*and Chemical Sciences Division, Lawrence Berkeley National Laboratory, Berkeley, California 94720*

(Received 18 April 2007; accepted 18 May 2007; published online 19 July 2007)

High resolution photoelectron spectra of the 1-propynyl and 1-propynyl-$d_3$ anions acquired with slow electron velocity-map imaging are presented. The electron affinity is determined to be $2.7355 \pm 0.0010$ eV for the 1-propynyl radical and $2.7300 \pm 0.0010$ eV for 1-propynyl-$d_3$. Several vibronic transitions are observed and assigned using the isotopic shifts and results from *ab initio* calculations. Good agreement between experimental spectra and calculations suggests a $C_{3v}$ geometry for the 1-propynyl radical. No evidence is found for strong vibronic coupling between the ground electronic state and the low-lying first excited state. © *2007 American Institute of Physics*. [DOI: 10.1063/1.2748399]

## INTRODUCTION

The 1-propynyl radical ($C{\equiv}C{-}CH_3$) is one of several stable $C_3H_3$ isomers.[1] The most stable of these, the propargyl radical ($HC{\equiv}C{-}CH_2$), has been well studied and characterized in detail.[2–9] It has been determined to be an important intermediate in interstellar chemistry,[10,11] hydrocarbon combustion,[12,13] and hydrocarbon photochemistry.[14–16] The other isomers have been the subject of several theoretical studies,[17–22] but owing to the fact that they all lie 30–40 kcal/mol higher in energy than propargyl, there is very little experimental information available on them. On the other hand, since the corresponding anions of the 1-propynyl and the propargyl radicals have similar energies[18] and selective isomer formation can be achieved using proper gas-phase chemistry,[23] anion photoelectron (PE) spectroscopy provides a straightforward means to access the energy levels of the energetic 1-propynyl radical.[3] In this paper, we show how a recently developed high resolution variant of anion PE spectroscopy, slow electron velocity-map imaging (SEVI),[24] can probe the vibronic structure of 1-propynyl in considerable detail.

Oakes and Ellison[2] set a lower bound of 2.60 eV to the electron affinity (EA) of the 1-propynyl radical based on the absence of photodetachment from the corresponding anion at 488 nm. The first anion PE spectrum of 1-propynyl was acquired by Robinson *et al.*[3] at 351 nm. Although several vibrationally resolved photodetachment transitions were seen, no assignment was attempted. An EA of 2.718 eV was determined using the lower peak of an apparent doublet at the origin transition. This doublet was attributed to a split of the degeneracy of the $^2E$ ground state in which the unpaired electron is in the $\pi$ orbital of the triple bond, based on the early theoretical work by Bauschlicher and Langhoff.[25] However, subsequent calculations[1,18–22,26] converged to a $^2A_1$ or $^2A'$ ground state with the unpaired electron in a nonbonding *sp* orbital on the terminal carbon. The "$\pi$" state has been calculated to be an extremely low-lying excited state with vertical excitation energy between 0.04 (Ref. 19) and 0.38 (Ref. 21) eV. The presence of such a low-lying degenerate excited state can cause artificial symmetry breaking of the wave function in single reference calculations and lead to distortion from the $C_{3v}$ geometry,[20,26] as has been seen in calculations on the $NO_3$ radical.[27] Moreover, possible combinations of Jahn-Teller and pseudo-Jahn-Teller effects can lead to a very complicated vibronic spectrum.[28]

In this paper, we present high resolution photodetachment spectra of the 1-propynyl and the 1-propynyl-$d_3$ anions acquired with the recently developed SEVI technique.[24] Several new vibronic transitions were resolved, and assignments were made aided by isotopic shifts and high-level *ab initio* calculations. It is shown that the apparent doublet at the origin transition in the previous PE study was from low-frequency sequence bands. Agreement between the harmonic calculation and the experimental spectra indicates at most weak vibronic coupling between the ground state and the first excited state of the 1-propynyl radical and a $C_{3v}$ geometry for both the anion and the radical.

## EXPERIMENT

The SEVI apparatus has been described in detail elsewhere.[24,29] The experiment is based on velocity-map imaging (VMI) of photoelectrons[30] using relatively low extraction voltages, with the goal of selectively detecting slow electrons with high efficiency and enlarging their image on the detector.

Briefly, anions formed by a pulsed molecular beam coupled to an electron source were perpendicularly extracted

[a)]Author to whom correspondence should be addressed. Electronic mail: dneumark@berkeley.edu

 

into a Wiley-McLaren time-of-flight mass spectrometer[31] and directed to the detachment region by a series of electrostatic lens and pinholes. A 1 $\mu$s pulse on the last ion deflector allowed only the desired mass into the interaction region. Anions were photodetached between the repeller and the extraction plates of the VMI stack by the focused output of a Nd:YAG pumped tunable dye laser. The photoelectron cloud formed was then coaxially extracted down a 50 cm flight tube and mapped onto a detector comprising a chevron-mounted pair of time-gated, image-quality microchannel plates coupled to a phosphor screen, as is typically used in photofragment imaging experiments.[32] Events on the screen were collected by a $1024 \times 1024$ charge-coupled device camera and sent to a computer. Electron velocity-mapped images resulting from 25 000 to 100 000 laser pulses were summed, quadrant symmetrized, and inverse-Abel transformed. Photoelectron spectra were obtained via angular integration of the transformed images.

The 1-propynyl (1-propynyl-$d_3$) anions were produced by expanding a 2% mixture of $NF_3$ in argon seeded with 1 Torr of 1-trimethylsilylpropyne (1-trimethylsilylpropyne-$d_3$) into the source vacuum chamber through an Even-Lavie pulsed valve[33] equipped with a circular ionizer. The 1-trimethylsilylpropyne (Aldrich) was used as received while 1-trimethylsilylpropyne-$d_3$ was synthesized according to standard procedure[34] and purified by freeze-pump-thaw cycles before use. Electron impact on $NF_3$ produces $F^-$ which then reacts with 1-trimethylsilylpropyne and selectively forms the 1-propynyl anion over the propargyl isomer due to the strength of the silicon-fluorine bond.[23]

$$CH_3C{\equiv}C-Si(CH_3)_3 + F^- \rightarrow CH_3C{\equiv}C^- + FSi(CH_3)_3.$$

Despite the use of this method, the formation of the propargyl anion is still possible via isomerization in the ionizing region. However, the propargyl radical has a much lower EA, 0.918 eV,[3] than 1-propynyl, and the SEVI detection scheme discriminates against the high energy photoelectrons from propargyl. In addition, the production of the propargyl anion could be minimized through the optimization of source conditions.

The apparatus was calibrated by acquiring SEVI images of atomic sulfur, which has six well known transitions within 1100 $cm^{-1}$ of each other.[35,36] Images were collected at several different photon energies for each repeller voltage used (100–350 V). In the 100 V images, the full width at half maximum (FWHM) of the peaks was 3.0 $cm^{-1}$ at 50 $cm^{-1}$ above threshold, while in the 350 V images the FWHM was 4.4 $cm^{-1}$ at 50 $cm^{-1}$ above threshold. In the SEVI experiment, applying a lower voltage on the repeller plate yields higher energy resolution. Also, within the same image, all observed transitions have similar widths in pixels ($\Delta r$), which means transitions observed further from threshold (larger $r$) are broader in energy.

## THEORETICAL METHODS

The complex electronic structure of the 1-propynyl anion and radical requires special attention when carrying out *ab initio* calculations. The anion has a closed-shell electronic wave function and can be treated with single reference methods. However, a diffuse atomic orbital basis and high-level treatment of electron correlation is necessary to achieve sufficient accuracy. The aug-cc-pVTZ basis was used for all calculations presented in this paper.[37,38] All calculations of the anion were performed using the restricted open-shell version of coupled-cluster theory with singles and doubles excitations including perturbative triples, abbreviated RCCSD(T).[39]

The neutral radical cannot be treated by this method because the electronic wave function suffers artificial symmetry breaking when treated at single reference level. This effect has been found before for symmetric open-shell systems; well known examples include $NO_3$ and $HCO_2$ (see Refs. 27 and 40 and references therein). The problem is solved by performing multireference configuration interaction (MRCI) calculations. First the reference orbitals are optimized at the complete active space self-consistent field (CASSCF) level of theory. These calculations are carried out in $C_s$ symmetry. The active space of the CASSCF calculations comprises four orbitals of $a'$ and two orbitals of $a''$ symmetry while seven $a'$ and one $a''$ orbitals are always kept doubly occupied. The electronic ground state and first excited state with $^2A_1$ and $^2E$ symmetries, respectively, are state averaged in these calculations. The reference configurations for the MRCI calculations are formed from the same active space. However, singles and doubles excitations are performed out of all occupied orbitals except the four lowest molecular orbitals of $a'$ symmetry. The calculations were performed with the internally contracted MRCI method[41,42] as implemented in MOLPRO.[43] All MRCI calculations include the multireference version of the Davidson correction.

Using the methods outlined above, the equilibrium geometries of the anion and radical ground states were optimized. For the excited state of the radical, only the $^2E_y(^2A'')$ component could be optimized due to a conical intersection between the $^2E_x(^2A')$ component and the ground state. Harmonic frequencies for both ground states were determined by diagonalizing the mass-weighted force constant matrix. The harmonic force field was obtained in symmetry coordinates and the normal mode analysis was carried out by an external program, making full use of the $C_{3v}$ symmetry. The results were utilized for the calculation of Franck-Condon factors and vibronic state energies in order to simulate the experimental spectra. All Franck-Condon integrals were calculated analytically, including Duschinsky rotation and distortion of the normal modes.[44–46]

The adiabatic photodetachment energy was calculated at RCCSD(T) level of theory since MRCI is not size extensive. For these calculations, exponential basis set extrapolations were performed for the reference, CCSD correlation, and perturbative triple energies, respectively. The 0-0 energies were obtained from the basis set limit and the harmonic zero-point energies.

## RESULTS

Figures 1-3 show SEVI spectra of $C_3H_3^-$ and $C_3D_3^-$. All spectra show electron signal as a function of electron binding

energy (eBE), defined as the difference between the photon energy and the measured electron kinetic energy,

$$\mathrm{eBE} = \mathrm{h}\nu - \mathrm{eKE}.$$

Figure 1 shows the PE spectrum[3] (panel I) and SEVI spectra (panels II and III) of the 1-propynyl anion. The trace in panel II was taken at 24 271.7 $cm^{-1}$ with a repeller voltage of 350 V; the insert shows a 10× base line zoom. The most intense feature in the spectrum is a single peak, labeled *A*, centered at 22 063 $cm^{-1}$. Panel III of Fig. 1 shows a 5× base line zoom of a spectrum taken at 23 096.1 $cm^{-1}$ and 250 V. The improved resolution in going to lower repeller voltage and closer to the detachment threshold can be clearly seen. The insert in panel III is an averaged trace of several 150 V images taken at slightly different wavelengths with 80 psi backing pressure, showing peak *A* near threshold at even higher resolution, where a partially resolved triplet feature with a 5–6 $cm^{-1}$ spacing was observed.

Transitions with lower eBE than peak *A* are labeled $b'-d'$ in Fig. 1, panel III. Peak $b'$, the most intense of these features, is centered at 21 937 $cm^{-1}$ with a width of 26 $cm^{-1}$. Transitions with higher eBE than peak *A* are labeled *B*–*J* in the panel II insert. The peaks have widths of 20–30 $cm^{-1}$, showing no obvious progression of vibrations. The most intense of these peaks are at 22 402(*B*) and 22 981(*E*) $cm^{-1}$. The highest eBE feature in Fig. 1 is at 24 081 $cm^{-1}$ (peak *J*); spectra taken at photon energies as high as 25 250.7 $cm^{-1}$ revealed no additional features.

Figure 2 shows SEVI spectra of 1-propynyl-$d_3$. These spectra share many similarities with those of $C_3H_3^-$. Peak *A*, the most intense feature, is centered at 22 019 $cm^{-1}$, with a FWHM of 21 $cm^{-1}$. The lower eBE peaks, $b'-d'$, are present with relative intensities similar to the $C_3H_3$ peaks. Again, peaks *B*–*J* lie within 2100 $cm^{-1}$ of peak *A*, with peaks *B* and *E* the more intense of these peaks, at 22 341 and 22 857 $cm^{-1}$, respectively. Spectra up to 25 124.1 $cm^{-1}$ were taken, but the highest eBE feature observed lies at 24 081 $cm^{-1}$ (*J*). Table I summarizes all the peaks observed in the SEVI experiments.

SEVI spectra of peaks $A-d'$ of $C_3H_3^-$ at different carrier gas backing pressures are shown in Fig. 3. The images were taken with a repeller voltage of 150 V at photon energies around 22 090 $cm^{-1}$. Higher backing pressure results in a cooler supersonic expansion and yields ions with more population in the ground rovibronic state. Figure 3 shows that as the backing pressure is raised, the relative intensities of peaks $b'-d'$ with respect to *A* decreases. Moreover, peak *A* narrows with increasing backing pressure, going from a width of 25 to 15 $cm^{-1}$, with a significant drop of the shoulder on the low eBE side. Similar behavior was observed for peaks $A-d'$ in $C_3D_3^-$ spectra.

To aid assignment of the spectra, *ab initio* results were obtained from the theoretical methods discussed in the computational section. Geometries for the anion and radical ground and first excited states are shown in Fig. 4; relatively small geometry changes upon photodetachment to either neutral state are found. The calculated EA for 1-propynyl is 22 490 $cm^{-1}$ (2.7884 eV). The *ab initio* adiabatic transition energy from the radical ground state to the first excited state

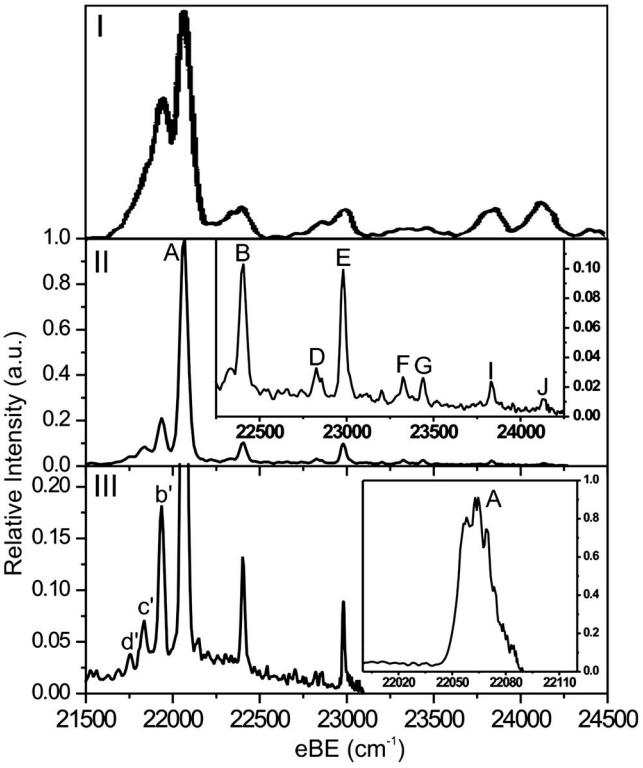


FIG. 1. Panel I shows the PE spectrum of $C_3H_3^-$ taken at photon wavelength of 351 nm (from Ref. 3). Panel II is a 350 V overview SEVI spectrum taken at 24 271.7 $cm^{-1}$; the insert shows a 10× base line zoom, indicating the vibrational peaks. Panel III shows a close to threshold SEVI spectrum for the first few vibrations, taken at 23 096.1 $cm^{-1}$ and 250 V repeller voltage. The bottom insert is an averaged 150 V with 80 psi backing pressure close to threshold SEVI spectrum of peak *A*.

was determined to be 1706 $cm^{-1}$. The equilibrium structure for the $^2E$ state is only slightly distorted from $C_{3v}$ symmetry, indicating only weak Jahn-Teller distortion. Table II lists the calculated vibrational frequencies of the anion and the neutral molecules, along with the frequencies for the deuterated species, and the corresponding isotope shift. Figure 5 com-

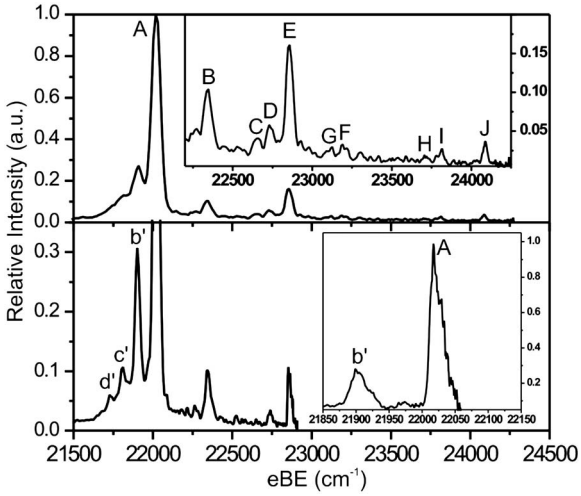


FIG. 2. SEVI spectra of $C_3D_3^-$. Top panel is a 350 V overview spectrum taken at 24 271.7 $cm^{-1}$; the insert shows a 5× base line zoom, indicating the vibrational peaks. Bottom panel shows a close to threshold spectrum for the first few vibrations, taken at 22 911.9 $cm^{-1}$ and 250 V repeller voltage. The bottom insert is an averaged 150 V close to threshold spectrum of peak *A*.

TABLE I. Peak position ($cm^{-1}$), isotope shifts ($cm^{-1}$), and assignments for the SEVI spectra of 1-propynyl and 1-propynyl-$d_3$. The uncertainties of the peak positions are ±10 $cm^{-1}$ (±20 $cm^{-1}$ where indicated with *).

| Peak | $C_3H_3$ eBE | $C_3H_3$ Shift from origin | $C_3D_3$ eBE | $C_3D_3$ Shift from origin | H/D shift | Assignment |
|---|---|---|---|---|---|---|
| *d'* | 21 760* | −303 | 21 732* | −287 | −16 | $8_3^3$ |
| *c'* | 21 836 | −227 | 21 812 | −207 | −20 | $8_2^2$ |
| *b'* | 21 937 | −126 | 21 903 | −116 | −10 | $8_1^1$ |
| *A* | 22 063 | 0 | 22 019 | 0 | 0 | $0_0^0(^2A)$ |
| *B* | 22 402 | 339 | 22 341 | 322 | 17 | $8_0^2$ |
| *C* | | | 22 653* | 634 | | $8_0^4$ |
| *D* | 22 848* | 785 | 22 744 | 725 | 60 | $4_0^1 8_1^1$ |
| *E* | 22 981 | 918 | 22 857 | 838 | 80 | $4_0^1$ |
| *F* | 23 327 | 1264 | 23 196* | 1177 | 87 | $4_0^1 8_0^2$ |
| *G* | 23 438 | 1375 | 23 112* | 1093 | 282 | $3_0^1$ |
| *H* | | | 23 674* | 1655 | | $4_0^2$ |
| *I* | 23 833 | 1770 | 23 807* | 1788 | −18 | $0_0^0(^2E)$ |
| *J* | 24 131 | 2068 | 24 081 | 2062 | 6 | $2_0^1$ |

pares the Franck-Condon (FC) simulation obtained from the theoretical results to the experiment. Agreement is good but not perfect; discrepancies are discussed below.

## DISCUSSION

The high resolution of the SEVI technique allows a closer look at the 1-propynyl radical than was available from the PE spectrum. The most intense feature in the SEVI spectra is peak *A*, which is assigned to the 0-0 origin band, giving an EA of 22 063±8 $cm^{-1}$ (2.7355±0.0010 eV) for the 1-propynyl radical. The *ab initio* result of 22 490 $cm^{-1}$ is in good agreement with experiment. The slightly higher computed EA may result from the $C_{3v}$ symmetrical reference wave function not being the lowest solution of the Hartree-Fock Hamiltonian due to artificial symmetry breaking in the radical at that level of theory.

The FWHM of peak *A*, at ~20 $cm^{-1}$, is larger than the instrumental resolution. The partially resolved triplet feature with an approximate spacing of 5 $cm^{-1}$ observed for this band indicates partly resolved rotational structure. This attribution is supported by the results of Fig. 3, which shows that peak *A* narrows as the backing pressure is raised, the expected result for colder rotational temperatures associated with higher backing pressures.

Peak *A* is broad enough to encompass parallel ($\Delta K=0$) transitions from populated $K''$ states and two perpendicular ($\Delta K=\pm 1$) transitions: $K'=1\leftarrow K''=0$ and $K'=0\leftarrow K''=1$. However, both perpendicular transitions are forbidden[47] because $K=0$ rovibronic levels have $A_1$ (even *J*) or $A_2$ (odd *J*) symmetry, while $K=1$ rovibronic levels have *E* symmetry.[48] Other perpendicular transitions such as $K'=2\leftarrow K''=1$ are allowed but would result in additional peaks well outside the peak *A* rotational profile, and were not observed in the SEVI experiment. Hence, the observed triplet is most likely due to the *P*, *Q*, and *R* branches of parallel transitions ($\Delta K=0$). Under this assumption, the calculated rotational profile is shown in Fig. 6, along with the averaged SEVI spectra taken at 80 psi. The simulation was done at 60 K using the *ab initio* rotational constants. The Hönl-London formulas[49] for line intensities of parallel transitions of a symmetric top molecule were utilized, but for each value of $K''$, the intensity of the *Q* branch was multiplied by a factor of 6 to match the

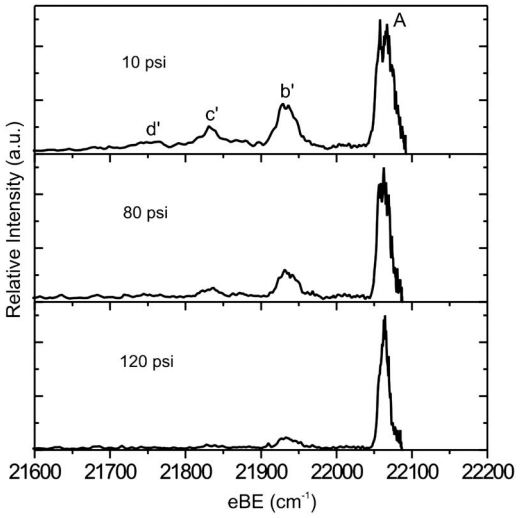


FIG. 3. Close to threshold spectra (150 V images) of the $C_3H_3$ origin peak taken at various backing pressures as indicated.

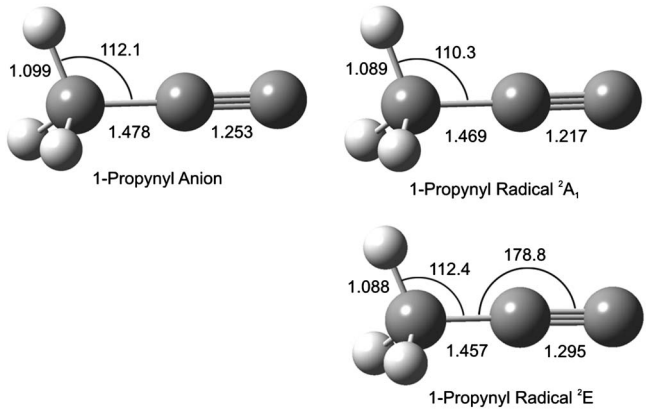


FIG. 4. *Ab initio* calculated geometries for the 1-propynyl radical (MRCI) and anion [RCCSD(T)].

TABLE II. Harmonic frequencies ($cm^{-1}$) and symmetries of $C_3H_3^-/C_3D_3^-$ [RCCSD(T)] and $C_3H_3/C_3D_3$ (MRCI) ground states, as well as isotope shifts ($cm^{-1}$) of the $C_3H_3$ vibrations.

| Mode | Symmetry | $C_3H_3^-$ | $C_3D_3^-$ | $C_3H_3$ | $C_3D_3$ | Radical H/D shift | |
|---|---|---|---|---|---|---|---|
| 1 | $A_1$ | 2964 | 2129 | 3069 | 2210 | 859 | $CH_3$ symmetric stretch |
| 2 | $A_1$ | 2000 | 1990 | 2177 | 2170 | 7 | C≡C stretch |
| 3 | $A_1$ | 1329 | 992 | 1428 | 1134 | 294 | $CH_3$ umbrella bend |
| 4 | $A_1$ | 729 | 709 | 937 | 853 | 84 | C–C stretch |
| 5 | $E$ | 2997 | 2217 | 3141 | 2325 | 816 | $CH_3$ asymmetric stretch |
| 6 | $E$ | 1492 | 1077 | 1501 | 1081 | 420 | HCH asymmetric bend |
| 7 | $E$ | 1039 | 821 | 1022 | 796 | 226 | CCH asymmetric bend |
| 8 | $E$ | 259 | 244 | 114 | 109 | 5 | CCC bend |

$C_3H_3^-$ rotational constants: $A=5.38\ cm^{-1}$ and $B=C=0.303\ cm^{-1}$
$C_3H_3$ rotational constants: $A=5.34\ cm^{-1}$ and $B=C=0.314\ cm^{-1}$
$C_3D_3^-$ rotational constants: $A=2.69\ cm^{-1}$ and $B=C=0.256\ cm^{-1}$
$C_3D_3$ rotational constants: $A=2.67\ cm^{-1}$ and $B=C=0.266\ cm^{-1}$

experimental result. This factor may result because the SEVI experiment involves direct detachment to a continuum rather than bound-bound electronic excitation.

For the 1-propynyl-$d_3$ radical, peak *A* is also the most intense feature in the spectrum. The EA was determined to be $22\,019\pm8\ cm^{-1}$ ($2.7300\pm0.0010$ eV), slightly redshifted compared to the protonated species. The *ab initio* result is $22\,444\ cm^{-1}$ (2.7809 eV), also showing a similar redshift compared to the calculated value for $C_3H_3$. There is no resolvable rotational structure for peak *A* in the $C_3D_3^-$ spectra, even though the width of this peak is comparable to the width of peak *A* in the $C_3H_3^-$ spectra.

We next consider the assignment of the vibrational features in the SEVI spectra. Assignments based on the following discussion are listed in Table I, while experimental fundamental frequencies are given in Table III.

There are several peaks due to vibrational transitions lying at higher eBE from the origin band, all of which are significantly weaker than the 0-0 transition. Low Franck-Condon activity is expected according to the calculations, as can be seen in the purely *ab initio* FC simulation in Fig. 5. Peaks *E* and *G* show good agreement in both position and relative intensity with the FC simulated transitions $4_0^1$ and $3_0^1$, respectively. Their isotope shifts also agree well with the calculated values, and therefore they are assigned to those transitions. Based on these assignments, the corresponding fundamental frequencies are given in Table III for both isotopomers. In the absence of anharmonicity, the $4_0^2$ overtone transition would occur at 1836 and 1676 $cm^{-1}$ in the $C_3H_3^-$ and $C_3D_3^-$ spectra, respectively. The very weak peak *H* in the $C_3D_3^-$ spectrum at 1655 $cm^{-1}$ from the origin thus appears to be the $4_0^2$ transition, but no corresponding feature is obvious in the $C_3H_3^-$ spectrum, presumably reflecting the low intensity of this transition.

Peak *B*, at 339 $cm^{-1}$ above the origin, shows an isotope shift of 17 $cm^{-1}$ upon deuteration. The closest calculated $C_3H_3$ vibrational frequency is 114 $cm^{-1}$ for the $\nu_8$ mode, corresponding to the degenerate C–C–C bend, which is almost a factor of 3 too low to assign peak *B* as the $8_0^1$ transi-

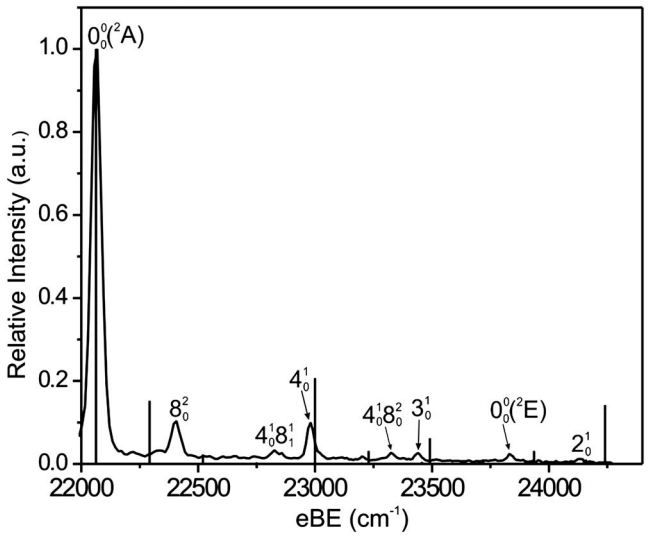


FIG. 5. Franck-Condon simulation of the $C_3H_3^-$ PE spectrum compared to the SEVI PE spectrum.

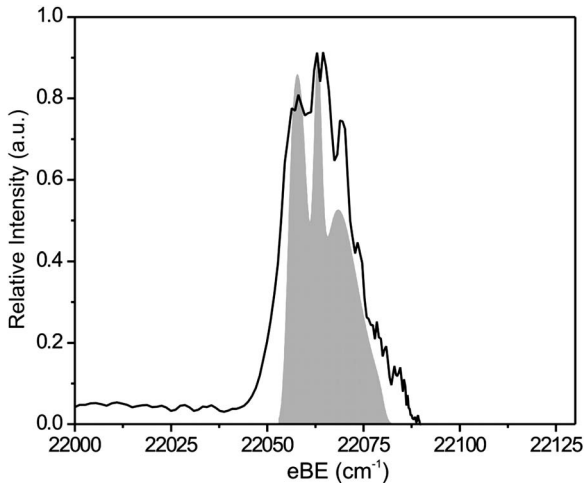


FIG. 6. Calculated rotational profile for the origin transition, compared to the averaged SEVI spectra taken at 80 psi backing pressure. The profile was calculated with the rotational constants from the *ab initio* results, at a temperature of 60 K.

TABLE III. Experimentally observed vibrational frequencies ($cm^{-1}$) of 1-propynyl and 1-propynyl-$d_3$ radicals and anions. Italics denote that fundamental vibrational frequency derived from overtone transitions.

| Mode | $C_3H_3^-$ | $C_3D_3^-$ | $C_3H_3$ | $C_3D_3$ |
|---|---|---|---|---|
| 1 | | | | |
| 2 | | | 2068 | 2062 |
| 3 | | | 1375 | 1093 |
| 4 | | | 918 | 838 |
| 5 | | | | |
| 6 | | | | |
| 7 | | | | |
| 8 | 295 | 277 | *169* | *161* |

tion. Such an assignment is problematic, in any case, since only even $\Delta\nu$ transitions are allowed for this non-totally symmetric vibration in the absence of vibronic coupling. On the other hand, the FC simulation in Fig. 5 shows a peak of similar intensity to *B* at 228 $cm^{-1}$ from the $8_0^2$ transition with a calculated isotope shift of 10 $cm^{-1}$. It appears more reasonable to assign peak *B* to this transition. The fundamental frequency of $\nu_8$ for the neutral is then derived to be approximately 169 $cm^{-1}$. This value is higher than the calculated fundamental frequency, a discrepancy perhaps reflecting that the harmonic approximation used in the calculation was not adequate in properly describing the flat potential of this low-frequency vibration. Peak *F*, at 1264 $cm^{-1}$ (1177 $cm^{-1}$ for $C_3D_3$) above the origin, is then assigned to the $4_0^1 8_0^2$ combination band based on its position and its isotope shift. The corresponding peak in the FC simulation is similarly redshifted as it was for peak *B*. Also, in the $C_3D_3^-$ spectrum, a very weak peak, *C*, is observed at approximately twice the frequency of *B* and is assigned to the $8_0^4$ transition.

The FC simulation indicates that the triple bond CC stretch, the totally symmetric $\nu_2$ mode with a calculated frequency of 2177 $cm^{-1}$, would have certain intensity in the SEVI spectrum. Peak *J*, at 2068 $cm^{-1}$ with only a 6 $cm^{-1}$ isotope shift, is assigned to the $2_0^1$ transition, only slightly redshifted compared to calculation. The relative intensity of this transition is higher in the FC simulation than in the SEVI spectra, because the cross section for photon absorption drops drastically as the energy above threshold approaches zero, as described by the Wigner threshold law.[50] In the previously recorded PE spectrum in Fig. 1 panel I, peak *J* has a similar intensity as peaks *B* and *E*.

Peak *I* is an interesting case. It lies in a region where the FC simulation shows only the $4_0^2$ transition. The $C_3D_3^-$ spectra show two features, *H* and *I*, in this spectral region, and the very small peak *H* has already been assigned to the $4_0^2$ transition. In the $C_3H_3^-$ spectra, only peak *I* is present at 1770 $cm^{-1}$ above origin. The $C_3H_3$ $\nu_4$ vibration has an experimental frequency of 918 $cm^{-1}$ (Table III), making peak *I* too far to the red for the $4_0^2$ assignment. Also, unlike all the other vibrational transitions, this peak blueshifted upon deuteration. Hence, peak *I* may be the transition to the low-lying $^2E$ excited electronic state of $C_3H_3$. This interpretation is consistent with the *ab initio* calculation of the adiabatic transition energy of 1706 $cm^{-1}$ for $C_3H_3$, in excellent agreement with the observed peak in question. However, the intensity of this peak is quite weak; even in Fig. 1 top panel (the previously reported PE spectrum), peak *I* is still weak compared to peak *A*. This anomalously low intensity may reflect a low photodetachment cross section to the $^2E$ state, similar to what was observed in the $NO_3^-$ PE spectrum,[51] where the photodetachment cross section to the ground electronic state was much lower than that to the first excited state.

On the lower eBE side of the origin band, there are several peaks, $b'-d'$, that have been assigned to transitions from vibrationally excited anions based on the temperature-dependent spectra in Fig. 3, which show that the relative intensities of these peaks decrease as the carrier gas backing pressure increases. As discussed earlier, higher backing pressure yields cooler ions with more population in the ground rovibronic state. The spectrum taken at 120 psi backing pressure has the smallest FWHM for band *A*, and correspondingly the lowest relative intensity for peaks $b'-d'$.

These peaks are readily assigned as sequence bands involving the $\nu_8$ mode. Peak $b'$, at −126 $cm^{-1}$ from the origin band, is the $8_1^1$ sequence band, and peak $c'$, at −227 $cm^{-1}$, is the $8_2^2$ transition. Peak $d'$ is very weak and is tentatively assigned to the $8_3^3$ sequence band. By using the experimental radical $\nu_8$ frequencies, the $\nu_8$ fundamental is found to be 295 $cm^{-1}$ in $C_3H_3^-$ and 277 $cm^{-1}$ for $C_3D_3^-$. The decreasing spacing in this series of peaks implies considerable anharmonicity in the C–C–C bend for the anion, perhaps reflecting that this mode promotes passage over the bent transition state for isomerization to the allenyl anion.[18] The isotope shifts of peaks $b'$ and $c'$ are consistent with these assignments, which also obey the even $\Delta\nu$ requirement for this non-totally symmetric vibration. Based on these assignments, the vibrational temperature of the molecules was estimated to be 230 K for 80 psi backing pressure. For both isotopomers, the spacing between peaks *D* and *E* is nearly the same as between $b'$ and *A*, so peak *D* is assigned to the $4_0^1 8_1^1$ transition.

The most intense of the sequence bands, peak $b'$, at 21 937 $cm^{-1}$ (2.7198 eV), corresponds to the previously determined EA of 2.718 eV, which was obtained from the PE spectrum reported by Robinson *et al.*[3] (Fig. 1, panel I). They observed a doublet at the apparent origin transition, which was attributed to a splitting of the nominally degenerate $^2E$ ground state. The electron affinity of 1-propynyl was then assigned to the lower eBE peak of the doublet. The SEVI study has shown that this assignment should be revised and that the actual 0-0 transition corresponds to the more intense, higher eBE peak of the doublet feature observed in the PE spectrum. In the SEVI spectra in Figs. 1–3, peak $b'$ is well resolved from the origin peak, clearly showing its low relative intensity and temperature dependence, both of which support its assignment to a hot band transition.

One expectation in this study was that the propynyl radical would exhibit interesting effects from pseudo-Jahn-Teller (pJT) coupling because of the close-lying $^2A_1$ and $^2E$ electronic states and that these could be probed using the high resolution of the SEVI technique. The strongest signature of pJT coupling is the presence of odd $\Delta\nu$ transitions in non-totally symmetric vibrational modes;[28] no such transitions were observed in our SEVI spectra. It thus appears that there is no obvious evidence for pJT effects in our spectra, and the

overall agreement between the experimental and calculated results points to a symmetric and undistorted ground state for the 1-propynyl radical.

We point out, however, that vibronic coupling in the radical may be observable with other techniques. Assuming our assignment of peak *I* to the $^2E$ state is correct, the photodetachment cross section to this state is extremely small and transitions allowed only by mixing with this state would be expected to be very weak. This situation is opposite to that found in the $NO_3^-$ photoelectron spectrum,[51] where nominally forbidden vibrational transitions in the ground state manifold are observed via coupling to an excited state that has a much larger photodetachment cross section.

## CONCLUSIONS

The high resolution SEVI spectra of the 1-propynyl radical have yielded a considerably improved electron affinity of $22\,063 \pm 8$ cm$^{-1}$ ($2.7355 \pm 0.0010$ eV). The EA of the 1-propynyl-$d_3$ is reported for the first time, with a value of $22\,019 \pm 8$ cm$^{-1}$ ($2.7300 \pm 0.0010$ eV). Vibrational assignments were made on the well resolved peaks. Activity in the $\nu_2$, $\nu_3$, $\nu_4$, and $\nu_8$ vibrations of the radical was observed, in accordance with Franck-Condon simulations, yielding fundamental frequencies for these modes in the neutral and for the $\nu_8$ mode in the anion. Based on the assignments, it is shown that the origin band of the radical is not split into a doublet but is in fact a single narrow band with partially resolved rotational features. The vibrational spectrum also showed little evidence for vibronic interactions, suggesting that the ground state of the radical is, as calculated, of $^2A_1$ symmetry. Possible evidence for the low-lying $^2E$ state was observed at 1770 cm$^{-1}$, a value in excellent agreement with the calculated adiabatic excitation energy.

## ACKNOWLEDGMENTS

One of the authors (D.M.N.) acknowledges support from the Air Force Office of Scientific Research under Grant No. F49620-03-1-0085. Another author (E.G.) thanks the National Science and Engineering Research Council of Canada for a postgraduate scholarship. The authors also acknowledge the help of Dr. Dubé for the synthesis of the 1-trimethylsilylpropyne-$d_3$ compound and are grateful to the *Leibniz Rechenzentrum Munich* for providing large amounts of computing time.

[1] T. L. Nguyen, A. M. Mebel, and R. I. Kaiser, J. Phys. Chem. A **105**, 3284 (2001).
[2] J. M. Oakes and G. B. Ellison, J. Am. Chem. Soc. **105**, 2969 (1983).
[3] M. S. Robinson, M. L. Polak, V. M. Bierbaum, C. H. Depuy, and W. C. Lineberger, J. Am. Chem. Soc. **117**, 6766 (1995).
[4] R. I. Kaiser, Y. T. Lee, and A. G. Suits, J. Chem. Phys. **105**, 8705 (1996).
[5] T. Gilbert, R. Pfab, I. Fischer, and P. Chen, J. Chem. Phys. **112**, 2575 (2000).
[6] J. C. Robinson, N. E. Sveum, and D. M. Neumark, J. Chem. Phys. **119**, 5311 (2003).
[7] J. A. Miller and S. J. Klippenstein, J. Phys. Chem. A **107**, 7783 (2003).
[8] L. R. McCunn, B. L. FitzPatrick, M. J. Krisch, L. J. Butler, C. W. Liang, and J. J. Lin, J. Chem. Phys. **125**, 133306 (2006).
[9] M. Wyss, E. Riaplov, and J. P. Maier, J. Chem. Phys. **114**, 10355 (2001).
[10] I. Cherchneff, J. R. Barker, and A. Tielens, Astrophys. J. **401**, 269 (1992).
[11] E. H. Wilson, S. K. Atreya, and A. Coustenis, J. Geophys. Res., [Planets] **108**, 5014 (2003).
[12] C. H. Wu and R. D. Kern, J. Phys. Chem. **91**, 6291 (1987).
[13] T. Zhang, X. N. Tang, K. C. Lau *et al.*, J. Chem. Phys. **124**, 074302 (2006).
[14] R. H. Qadiri, E. J. Feltham, E. E. H. Cottrill, N. Taniguchi, and M. N. R. Ashfold, J. Chem. Phys. **116**, 906 (2002).
[15] A. Fahr and A. H. Laufer, J. Phys. Chem. A **109**, 2534 (2005).
[16] J. C. Robinson, N. E. Sveum, S. J. Goncher, and D. M. Neumark, Mol. Phys. **103**, 1765 (2005).
[17] G. J. Collin, H. Deslauriers, G. R. Demare, and R. A. Poirier, J. Phys. Chem. **94**, 134 (1990).
[18] S. Ikuta, J. Mol. Struct.: THEOCHEM **434**, 121 (1998).
[19] A. M. Mebel, W. M. Jackson, A. H. H. Chang, and S. H. Lin, J. Am. Chem. Soc. **120**, 5751 (1998).
[20] L. Vereecken, K. Pierloot, and J. Peeters, J. Chem. Phys. **108**, 1068 (1998).
[21] W. Eisfeld, Phys. Chem. Chem. Phys. **7**, 3924 (2005).
[22] S. E. Wheeler, K. A. Robertson, W. D. Allen, H. F. Schaefer, Y. J. Bomble, and J. F. Stanton, J. Phys. Chem. A **111**, 3819 (2007).
[23] C. H. Depuy, V. M. Bierbaum, L. A. Flippin, J. J. Grabowski, G. K. King, and R. J. Schmitt, J. Am. Chem. Soc. **101**, 6443 (1979).
[24] A. Osterwalder, M. J. Nee, J. Zhou, and D. M. Neumark, J. Chem. Phys. **121**, 6317 (2004).
[25] C. W. Bauschlicher and S. R. Langhoff, Chem. Phys. Lett. **193**, 380 (1992).
[26] R. K. Sreeruttun, P. Ramasami, C. S. Wannere, A. Paul, P. V. R. Schleyer, and H. F. Schaefer, J. Org. Chem. **70**, 8676 (2005).
[27] W. Eisfeld and K. Morokuma, J. Chem. Phys. **113**, 5587 (2000).
[28] H. Köppel, W. Domcke, and L. S. Cederbaum, Adv. Chem. Phys. **57**, 59 (1984).
[29] M. J. Nee, A. Osterwalder, J. Zhou, and D. M. Neumark, J. Chem. Phys. **125**, 014306 (2006).
[30] A. T. J. B. Eppink and D. H. Parker, Rev. Sci. Instrum. **68**, 3477 (1997).
[31] W. C. Wiley and I. H. McLaren, Rev. Sci. Instrum. **26**, 1150 (1955).
[32] D. W. Chandler and P. L. Houston, J. Chem. Phys. **87**, 1445 (1987).
[33] U. Even, J. Jortner, D. Noy, N. Lavie, and C. Cossart-Magos, J. Chem. Phys. **112**, 8068 (2000).
[34] K. S. Feldman and D. A. Mareska, J. Org. Chem. **64**, 5650 (1999).
[35] W. C. Lineberger and B. W. Woodward, Phys. Rev. Lett. **25**, 424 (1970).
[36] C. E. Moore, *Atomic Energy Levels* (U.S. GPO, Washington, DC, 1958), Vol. III.
[37] T. H. Dunning, J. Chem. Phys. **90**, 1007 (1989).
[38] R. A. Kendall, T. H. Dunning, and R. J. Harrison, J. Chem. Phys. **96**, 6796 (1992).
[39] P. J. Knowles, C. Hampel, and H. J. Werner, J. Chem. Phys. **99**, 5219 (1993).
[40] E. H. Kim, S. E. Bradforth, D. W. Arnold, R. B. Metz, and D. M. Neumark, J. Chem. Phys. **103**, 7801 (1995).
[41] H. J. Werner and P. J. Knowles, J. Chem. Phys. **89**, 5803 (1988).
[42] P. J. Knowles and H. J. Werner, Chem. Phys. Lett. **145**, 514 (1988).
[43] http://www.molpro.net
[44] T. E. Sharp and H. M. Rosenstock, J. Chem. Phys. **41**, 3453 (1964).
[45] E. V. Doktorov, I. A. Malkin, and V. I. Manko, J. Mol. Spectrosc. **56**, 1 (1975).
[46] E. V. Doktorov, I. A. Malkin, and V. I. Manko, J. Mol. Spectrosc. **64**, 302 (1977).
[47] R. Signorell and F. Merkt, Mol. Phys. **92**, 793 (1997).
[48] P. R. Bunker and P. Jensen, *Molecular Symmetry and Spectroscopy*, 2nd ed. (NRC Research, Ottawa, 1998).
[49] H. Hönl and F. London, Z. Phys. **33**, 803 (1925).
[50] E. P. Wigner, Phys. Rev. **73**, 1002 (1948).
[51] A. Weaver, D. W. Arnold, S. E. Bradforth, and D. M. Neumark, J. Chem. Phys. **94**, 1740 (1991).